Radiotherapy and Oncology 133 (2019) 120–124

Contents lists available at ScienceDirect

Radiotherapy and Oncology

journal homepage: www.thegreenjournal.com

Orignal Article

Intrinsic and extrinsic tumor characteristics are of minor relevance for the efficacy of split-dose carbon ion irradiation in three experimental prostate tumors

Christin Glowa [a,b,e,*], Peter Peschke [b,e], Stephan Brons [d,e], Jürgen Debus [a,c,e], Christian P. Karger [b,e]

[a] Department of Radiation Oncology and Radiotherapy, University Hospital Heidelberg; [b] Department of Medical Physics in Radiation Oncology, German Cancer Research Center (DKFZ); [c] Clinical Cooperation Unit Radiation Therapy, German Cancer Research Center (DKFZ); [d] Heidelberg Ion Beam Therapy Center (HIT); and [e] Heidelberg Institute for Radiation Oncology (HIRO), National Center for Radiation Research in Oncology (NCRO), Heidelberg, Germany

ARTICLE INFO

Article history:
Received 26 June 2018
Received in revised form 30 October 2018
Accepted 18 December 2018
Available online 24 January 2019

Keywords:
Carbon ion radiotherapy
Relative biological effectiveness (RBE)
Prostate tumor
Tumor heterogeneity

ABSTRACT

Objective: To quantify the impact of tumor-associated resistance factors on local tumor control after split doses of carbon (^{12}C-) ions or photons in an experimental prostate tumor model.
Material and methods: Three sublines (AT1, H, HI) of syngeneic rat prostate tumors (R3327) differing in growth rate, differentiation and hypoxic status were irradiated with split doses of either ^{12}C-ions or 6 MV photons. Dose–response curves were determined for the endpoint local tumor control within 300 days. The relative biological effectiveness (RBE) of ^{12}C-ions was calculated from the TCD_{50}-values (dose at 50% control probability) of photons and ^{12}C-ions.
Results: Experimental findings demonstrated: (i) The RBE was highest for the least differentiated AT1-tumor (2.39 ± 0.16 (AT1) vs 2.06 ± 0.11 (H) and 2.03 ± 0.17 (HI)). (ii) TCD_{50}-values between the three tumor sublines differed much less for ^{12}C-ions (26.0–37.9 Gy) than for photons (53.7–90.6 Gy). (iii) While the slope of the dose–response curves for photons and ^{12}C-ions were very similar for the AT1- and H-tumors, the histologically heterogeneous HI-tumor showed a shallow dose–response curve for photons, which is transformed into a steep dose–response curve after ^{12}C-ion irradiation.
Conclusion: The response to carbon ion irradiations is much less dependent on biological differences between and within the tumor-sublines. Tumors showing a high resistance against photon treatments, also exhibit the largest RBE for carbon ions. Carbon ions could therefore be of clinical advantage for the treatment of tumors with known resistance factors against photons.
 Radiotherapy and Oncology 133 (2019) 120–124

One of the major strategies for the treatment of inoperable localized solid tumors is radiotherapy with high-energy photons, however, in some cases radioresistant tumor cells survive and lead to tumor recurrence. Due to the tolerance of the adjacent normal tissue, dose escalation is usually not possible. Radiotherapy with carbon (^{12}C)-ions[1] allows for highly conformal irradiations due to the advantageous depth dose curve (Bragg-peak) and the increased linear energy transfer (LET) of ^{12}C-ions, leading to an increased relative biological effectiveness (RBE) with respect to photons. While the conformity is used to increase the sparing of the surrounding normal tissue [1], the higher LET in the target volume is expected to enhance the treatment effectiveness in the tumor. The reason for the increased effectiveness is caused by a larger number of clustered DNA damages originating from the high local energy deposition of ^{12}C-ions [2,3]. This difference in the damage pattern leads to an increased RBE of ^{12}C-ions as compared to photons [4,5] and it is hypothesized that this can be used to improve clinical outcome.

Clinical studies of carbon ion radiotherapy from Japan [6–9] and Germany [10–15] revealed high local tumor control rates for different tumor entities, however, final results of prospective clinical trials are still pending and the selection of the most promising tumor entities is still under discussion. Stratification of patients is especially important as there are only very few carbon ion facilities available worldwide (https://www.ptcog.ch/).

To better understand the effectiveness of ^{12}C-ion therapy, *in vitro* studies have been performed resulting in RBE-values for many cell lines [16], but only very few studies were carried out quantifying the RBE in experimental tumor systems [17–23]. While

* Corresponding author at: German Cancer Research Center (DKFZ), Dept. of Medical Physics in Radiation Oncology (E040), Im Neuenheimer Feld 280, 69120 Heidelberg, Germany.
E-mail addresses: c.glowa@dkfz.de (C. Glowa), p.peschke@dkfz.de (P. Peschke), Stephan.Brons@med.uni-heidelberg.de (S. Brons), juergen.debus@med.uni-heidelberg.de (J. Debus), c.karger@dkfz.de (C.P. Karger).

[1] ^{12}C-ions: carbon ions; CI: confidence interval; LET: linear energy transfer; RBE: relative biological effectiveness; SOBP: Spread-out-Bragg-peak; TCD_{50}-value: dose at 50% control probability

https://doi.org/10.1016/j.radonc.2018.12.017
0167-8140/

most of them analyzed the fractionation dependence of the RBE, only one single fraction study investigated different tumor sublines of the same tumor to study the impact of tumor-specific factors [22]. For this, three sublines of the very well-characterized prostate carcinoma R3327 differing in growth rate, differentiation and hypoxic status were used together with the endpoint local control [24]. The present study extends this investigation to split doses to analyze the impact of these biological factors under fractionation.

Material and methods

Tumor model

Fresh fragments of tumor tissue of the syngeneic Dunning prostate adenocarcinoma sublines R3327-H, -HI and -AT1 [24] were implanted subcutaneously in the distal thigh of young adult male Copenhagen rats (weight 180–200 g, Charles River Laboratories, Wilmington, Massachusetts, USA). During irradiation of H- and HI-tumors, rats were kept under inhalation anesthesia with a mixture of 2.5% sevoflurane (Abbott, Wiesbaden, Germany) and oxygen at 2 l/min using an inhalation mask. Anesthesia of the AT1-study has been described previously [19]. All experiments were approved by the governmental review committee on animal care (Ref. No. 35-9185.81/G-43/11), and animals were kept under standard laboratory conditions.

Irradiation setup

The AT1 study has been published previously [19,20] and the experimental setup for H and HI in this study is the same. Rats were placed in a special device for accurate positioning of the tumor (see details in [19]. The mean tumor diameter at treatment was 11 mm (range 9.0–12.5 mm). Photon irradiations were performed using a single 6 MV beam of a linear accelerator (Siemens, Erlangen, Germany) and the field size was shaped by a cylindrical tungsten collimator (90% isodose: 15 mm at the isocenter). For ^{12}C-ions, the tumor was positioned at the center of a single 20 mm spread-out-Bragg-peak (SOBP) having a field size of 18×18 mm^2. The mean dose-averaged LET in the tumor was 75 keV/μm (range 64–96 keV/ μm).

In the present study, 165 animals were irradiated on consecutive days with increasing equally weighted split doses of photons or ^{12}C-ions, respectively (Table 1). 24 sham-treated animals served as controls. Primary endpoint was local tumor control within 300 days, defined as no detectable tumor regrowth. Tumor volume was measured routinely using a caliper [19]. While locally controlled AT1- and HI-tumors regressed completely, residual fibrotic nodules remained in case of locally controlled H-tumors. Therefore, "histological control" at 300 days defined as fibrotic pattern without proliferation (BrdU) was used as secondary endpoint for locally controlled H-tumors.

Statistical analysis

For the primary endpoint "local tumor control", actuarial control rates were calculated and the logistic dose–response model was fitted using the maximum likelihood fitting procedure of the software STATISTICA (version 10.0, Statsoft Inc., www.statsoft.com) (see [22] for details). Incomplete follow-up of animals was considered in the fitting procedure using the method of effective sample sizes that corrects the number of treated and responding tumors to match actuarial response rates and their variances [25]. For the endpoint "histological tumor control", no actuarial approach was required as surviving (i.e. proliferating) tumor cells were directly detected by the proliferation marker BrdU. In this case the dose–response model was adjusted to the experimentally observed incident rates. For both endpoints, the RBE was calculated as the ratio of the TCD_{50}-values (dose at 50% tumor control probability) for photons and ^{12}C-ions. Standard errors of TCD_{50} and RBE were calculated by error propagation. For TCD_{50}, the correlation of the fit parameters was considered. In addition, 90% confidence intervals (CIs) were calculated using Fieller's theorem [26].

Table 1
Dose levels and number of animals in the experiment.

Experiment	Dose levels [Gy] (animals per dose level)	Animals
H-Tumor		
Photons	35 (5), 40 (5), 45 (5), 50 (6), 55 (5), 60 (5), 65 (5), 70 (5), 75 (5[#,+]), 80 (3)	49
^{12}C-ions	16 (5), 20 (5), 24 (5), 28 (5), 32 (5), 36 (5[#,+]), 40 (5), 44 (5)	40
Controls	6 sham-treated tumors per experimental arm	12
HI-Tumor		
Photons	55 (3), 60 (5), 65 (5), 70 (6[*]), 75 (6[*,++]), 80 (8[*]), 85 (6), 90 (7[*]), 95 (5[§])	51
^{12}C-ions	29 (3), 33 (6), 37 (6[#]), 41 (6), 45 (4)	25
Controls	6 sham-treated tumors per experimental arm	12
Total		**189**

[#] One animal died due to unknown reasons.
[*] One animal died due to metastases.
[+] No histology in one animal.
[++] No histology in two animals.
[§] 2 animals died due to metastases.

Histology

For evaluation of the remaining tumor structure in irradiated H-tumors, Hematoxylin & Eosin staining (Carl Roth, Karlsruhe, Germany) was performed on cryo-preserved sections [22]. In addition, Cryo-preserved methanol/acetone fixed sections were stained for proliferating cells using a BrdU antibody (Roche Diagnostics, Mannheim, Germany). Prior to sacrificing, BrdU (100 mg/kg, Sigma-Aldrich, Taufkirchen, Germany) was injected intraperitoneally. The complete staining procedure has been described in [22].

Results

Fig. 1 shows the adjusted dose-response curves for the three tumor sublines. The resulting TCD_{50}- and RBE-values are displayed in Table 2. These results revealed three important findings:

(i) Comparing the dose–response curves of the three tumor sublines for the primary endpoint local tumor control (Fig. 1), the more differentiated H- and HI-tumors showed comparable RBEs (2.06 ± 0.11 and 2.03 ± 0.17, respectively), whereas a markedly increased RBE was found for the anaplastic AT1-tumor (2.39 ± 0.16). While locally controlled AT1- and HI-tumors regressed completely, tiny nodules remained in case of locally controlled H-tumors. Using histological tumor control as secondary endpoint shifted the TCD_{50}-values by 9.3 Gy for photons and 8.4 Gy for ^{12}C-ions (Fig. 1a) and the related RBE decreased to 1.83 ± 0.12. Replacing the RBE of the H-tumor by this value, results in a systematic increase of the RBE with decreasing differentiation. The late recurrence of a single HI tumor at 388 days for ^{12}C-ions altered the TCD_{50}- and RBE-values only marginally (Fig. 1b, dashed line).

(ii) TCD_{50}-values between the three tumor sublines differed much less for ^{12}C-ions (26.0–37.9 Gy) than for photons (53.7-90.6 Gy) (Fig. 2a). For ^{12}C-ions, only the H-tumor showed a significantly lower TCD_{50}, however, if this value is replaced by that for the endpoint histological tumor control, the range of TCD_{50}-values is reduced to (34.4-37.9 Gy), while that for photons is still very large (63.9-90.6 Gy) (Fig. 2b).

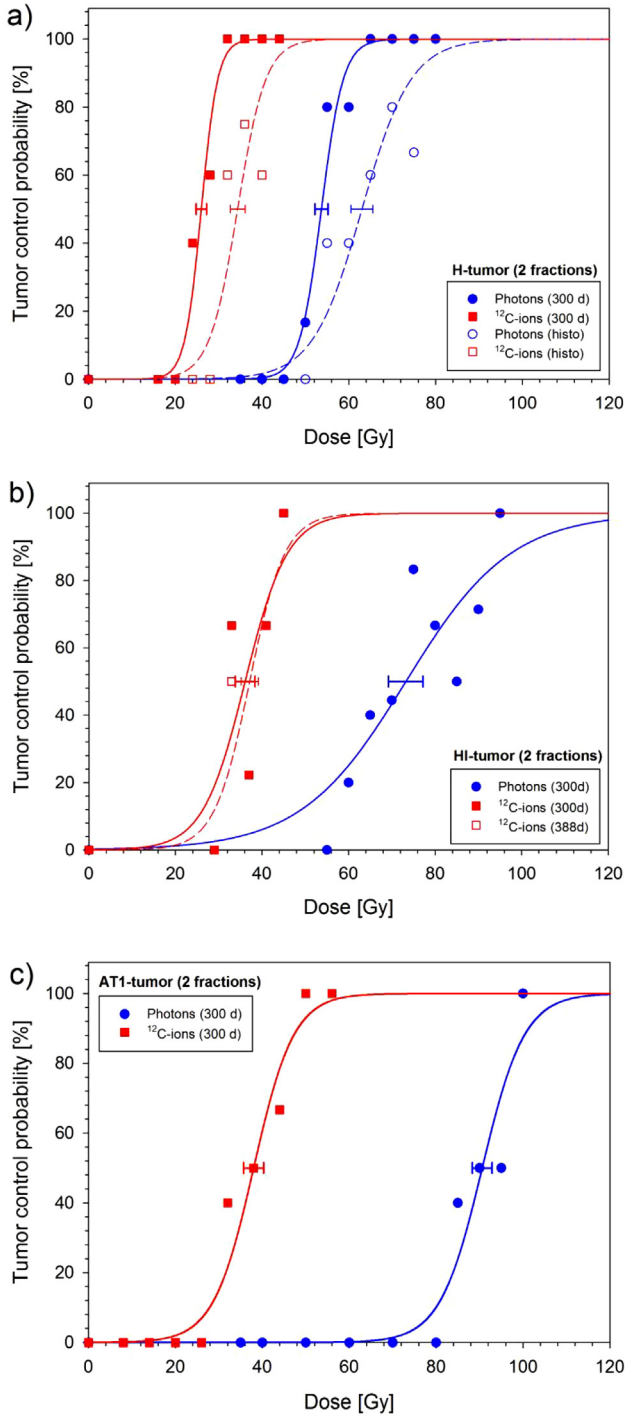

Fig. 1. Dose–response curves of the three sublines of the R3327 prostate carcinoma after split doses on consecutive days of photons (blue) and ^{12}C-ions (red), respectively. Error bars indicate the uncertainty of TCD_{50} (1 SD). Solid lines refer to the primary endpoint "local tumor control within 300 d". For the H-tumor (a), the dose–response curves for the secondary endpoint "histological control" are additionally shown. For the HI-tumor (b), a single ^{12}C-treated tumor regressed at 388 d, which however, lead only to a minor difference in the dose–response curve (dashed line). For 24 HI-tumors (12 per radiation modality), which were locally controlled at 300 days, the follow-up was extended to 400 days to check for late recurrences. For comparison, the previously measured dose–response curves for the AT1-tumor (c) are also displayed [20]. (For interpretation of the references to colour in this figure legend, the reader is referred to the web version of this article.)

Table 2
TCD_{50}-and RBE-values for three tumor sublines of the R3327 prostate carcinoma measured in this and a previous study, including single standard errors and 90%-confidence intervals. Endpoints for this dose–response study were "local tumor control (LC) within 300 d" or "histological tumor control" (Histo). As one single HI-tumor recurred later than 300 d, TCD_{50} at 388 d was additionally calculated for the primary endpoint.

Endpoint	TCD_{50} ± SE [Gy]		RBE ± SE *(90% CI)*
	Photons	^{12}C-ions	
H-Tumor (this study)			
LC (300 d)	53.7 ± 1.5	26.0 ± 1.2	2.06 ± 0.11 *(1.89–2.27)*
Histo	63.0 ± 2.5	34.4 ± 1.7	1.83 ± 0.12 *(1.65–2.24)*
HI-Tumor (this study)			
LC (300 d)	73.2 ± 4.0	36.1 ± 2.3	2.03 ± 0.17 *(1.77–2.33)*
LC (388 d)	73.2 ± 4.0	37.2 ± 2.0	1.97 ± 0.15 *(1.74–2.23)*
AT1-Tumor [20]			
LC (300 d)	90.6 ± 2.3	37.9 ± 2.3	2.39 ± 0.16 *(2.15–2.68)*

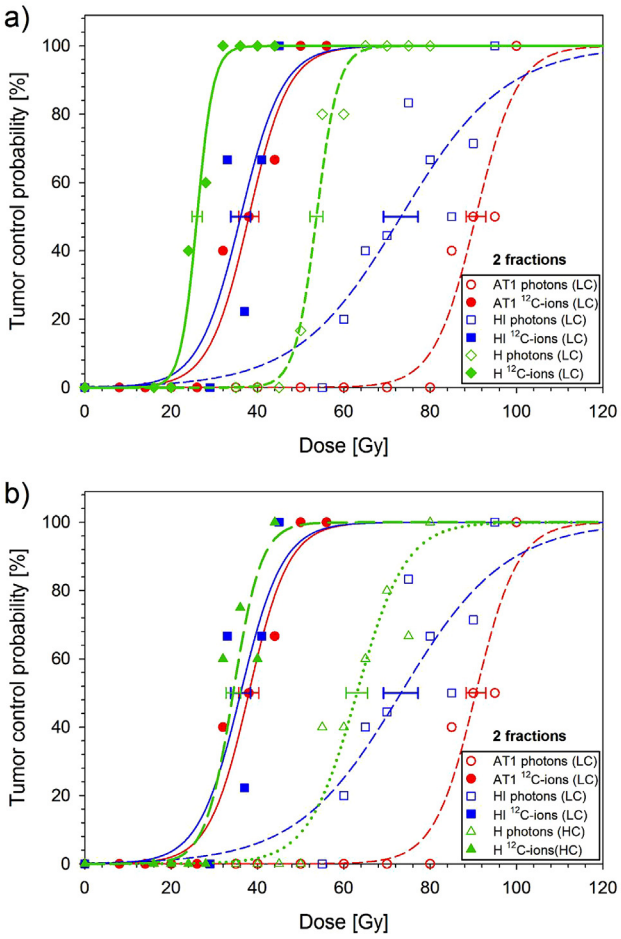

Fig. 2. Compilation of dose–response curves employing (a) the primary endpoint local control (LC) for all three tumor-sublines and (b) the endpoints LC for the AT1- and HI-tumors and the endpoint histological control (HC) for the H-tumor.

(iii) While the slope of the dose–response curves for photons and ^{12}C-ions were very similar for the histologically homogeneous AT1- and H-tumors, the histologically heterogeneous HI-tumor showed a much steeper dose–response curve for ^{12}C-ions than for photons (Fig. 2). This finding was independent of the considered biological endpoint.

Discussion

This is the first fractionated study that investigates the RBE for different sublines of the same tumor, which differ in several tumor-specific factors. Besides histological differentiation, another

important factor is the hypoxic status, which is known to impact the response to radiotherapy. While the H-tumor is well oxygenated, the HI-tumor exhibits a moderately and mostly acute hypoxic pattern. In contrast, the anaplastic AT1-tumor presents a large fraction of poorly perfused immature vessels leading to chronic hypoxic regions, which explains the higher resistance against photon treatments [22,27].

The present study uses local tumor control as primary endpoint. In contrast to growth delay, this requires high therapeutic doses that sterilize not only the majority of tumor cells but also small sub-populations of potentially radioresistant, e.g. quiescent, cells. With this respect, the required follow-up time is guided by the volume-doubling-time and the assessment whether a tumor is locally controlled additionally depends on the regression characteristics of controlled tumors. For the relatively fast growing AT1- and HI-tumors, this assessment turned out to be very reliable as the tumors regressed completely and even for the slower growing HI-tumors, only one locally controlled tumor regressed after the end of follow-up. For H-tumors, however, small nodules remained in apparently controlled tumors. As a potential regrowth of these nodules would occur beyond feasible observation times, due to the large doubling time of the H-tumor, the secondary endpoint "histological control" was used to quantify the robustness of the primary endpoint "local control" assuming that only proliferative active tumor cells can lead to a regrowth of the tumor while this is not the case for solely fibrotic nodules.

The primary endpoint revealed the highest RBE for the anaplastic AT1-tumor and indicated no relevant difference between the HI- and H-tumor. This result was essentially maintained, when replacing the endpoint local tumor control by histological tumor control for the H-tumor. A similar result was obtained in our previous single fraction study, where we found an increase of the RBE with decreasing differentiation independent of the considered endpoint [22]. This may be taken as important selection criteria for carbon ion treatments. Comparing the TCD_{50}-values of the present and the previous study, it is worth noticing that the fractionation ratios for photons and carbon ions turned out to be very similar (1.15-1.20 for the AT1- and HI- and 1.28-1.30 for the H-tumor). Thus fractionation seems to matter less for the investigated fractional doses.

A limitation of our study, however, are the high fractional doses as the induced vessel damage, the potential of reoxygenation, the induction of other microenvironmental factors as well as the immune response could be very different from that of the conventionally used low fractional doses. Nevertheless, this study is a first step to evaluate the fractionation effects of these three tumor sublines for photon and ^{12}C-ion irradiation. Further experiments at lower fractional doses are required. In addition, the LET in our 1 cm tumors was relatively high and rather uniformly distributed while this is not the case for larger clinical tumors, unless special measures like LET-painting [28] are taken into account. Larger tumors may also have more extended hypoxic areas as compared to experimental tumors. Nonetheless, our study provides important information on the effect of high-LET radiation on tumors with different hypoxic and histological characteristics. Finally, although tolerance doses at higher effect levels might be considered clinically more relevant, TCD_{50} is the most stable response parameter with the smallest uncertainty and it is not expected that this choice affects the conclusions of the study.

Regarding the absolute values of the TCD_{50}, it is striking that the RBE-differences between the three tumor sublines originate mainly from differences in the photon response, while the dose-response curves for ^{12}C-ions remain stable in a very narrow range. This range is even further decreased to only 3.5 Gy, when using histological rather than local control as endpoint for the H-tumor. Considering the histological study endpoint, an identical effect was observed in our previous single dose study [22], where the dose range for carbon ions was squeezed from 23.6-32.9 Gy to 26.8-32.9 Gy, while the range for photons still remained extremely large (48.3-75.7 Gy). This leads to the important conclusion, that the response to ^{12}C-ion irradiation is largely independent of tumor-specific factors like cell differentiation, hypoxia and proliferation rate. This holds true for single as well as for split dose irradiations. This finding indicates that there is significant uncertainty in the dependence of local control on tumor differentiation after photon treatments whereas this uncertainty is drastically reduced for carbon ions.

The results for single and split dose are also comparable with respect to the slope of the dose-response curves for photons and ^{12}C-ions [22]. While the fast growing AT1-tumor as well as the slow growing H-tumor exhibit steeply raising dose–response curves, the slope for the HI-tumor is much shallower for photons as compared to ^{12}C-ions. On the histological level, AT1-tumors predominantly consist of anaplastic tumor cells, H-tumors are characterized by few tumor cells spread within highly differentiated normal prostate structures, while HI-tumors are composed of a varying mixture of tumor and normal tissues, resulting in a more pronounced inter-tumoral variability [22,29]. Based on the assumption that the slope of dose-response curves reflects inter-tumoral variability, this leads to the conclusion that the impact of this variability on the population-based tumor response is reduced for ^{12}C-ions. Patient-to-patient variations of tumor-radiosensitivity can therefore be expected to be of reduced clinical relevance for ^{12}C-ions.

Regarding the response heterogeneity between and within the different tumor sublines, it was not possible to uniquely identify the specific biological factor, which affects the response to photon irradiation most as *in vivo* all potential factors act simultaneously. Based on previous investigations, however, some important factors may be specified: epigenetic alterations during the process of tumor dedifferentiation [24], discrepancies with respect to extent, pattern and dynamics of hypoxia [29–31], and differences in potential cancer stem cells within the three tumor sublines [32]. Each of these factors could contribute to the differential radioresistance of the three tumor sublines against photon irradiations.

In summary, it can be concluded that the differential fractionation effect between ^{12}C-ions and photons is only marginal for the investigated fractional doses. Moreover, the response to ^{12}C-ion irradiation is much less dependent on biological differences between and within tumors. The observation that radioresistance appears as a feature of the photon irradiation, explains the finding that the tumors with the highest resistance against photon treatments exhibit also the largest RBE for ^{12}C-ions. Translated to the clinical situation, the response to ^{12}C-ions is less dependent on tumor heterogeneity and could therefore be of great advantage for the treatment of neoplasms with actual or potential resistance factors against photons. Although this experimental finding has still to be confirmed clinically, it is interesting to note that a Japanese trial found comparably high 5-year local control rates for low-, intermediate- and high-risk prostate cancer patients treated with ^{12}C-ions [33].

Financial support

This study was supported by Deutsche Forschungsgemeinschaft (DFG, KFO 214).

Conflict of interest

The authors disclose no potential conflicts of interest.

Acknowledgement

The authors are grateful to Prof. Eric Hahn for his valuable hints regarding the experiment design and to the staff of the Heidelberg Ion Therapy Center (HIT) for providing excellent working conditions. This work was supported by the German Research Foundation (DFG, KFO 214).

References

[1] Combs SE, Debus J. Treatment with heavy charged particles: systematic review of clinical data and current clinical (comparative) trials. Acta Oncol 2013;52:1272–86.
[2] Tobias F, Durante M, Taucher-Scholz G, Jakob B. Spatiotemporal analysis of DNA repair using charged particle radiation. Mutat Res 2010;704:54–60.
[3] Hagiwara Y, Niimi A, Isono M, et al. 3D-structured illumination microscopy reveals clustered DNA double-strand break formation in widespread gammaH2AX foci after high LET heavy-ion particle radiation. Oncotarget 2017;8:109370–81.
[4] Held KD, Kawamura H, Kaminuma T, et al. Effects of charged particles on human tumor cells. Front Oncol 2016;6:23. https://doi.org/10.3389/fonc.2016.00023.
[5] Karger CP, Peschke P. RBE and related modeling in carbon-ion therapy. Phys Med Biol 2017;63. https://doi.org/10.1088/1361-6560/aa9102. 01TR02.
[6] Kamada T. Clinical evidence of particle beam therapy (carbon). Int J Clin Oncol 2012;17:85–8.
[7] Kamada T, Tsujii H, Blakely EA, et al. Carbon ion radiotherapy in Japan: an assessment of 20 years of clinical experience. Lancet Oncol 2015;16:e93–e100.
[8] Mohamad O, Makishima H, Kamada T. Evolution of carbon ion radiotherapy at the national institute of radiological sciences in Japan. Cancers 2018;10. https://doi.org/10.3390/cancers10030066.
[9] Kawashiro S, Yamada S, Isozaki Y, Nemoto K, Tsuji H, Kamada T. Carbon-ion radiotherapy for locoregional recurrence after primary surgery for pancreatic cancer. Radiother Oncol 2018;129:101–4. https://doi.org/10.1016/j.radonc.2018.02.003.
[10] Combs SE, Kessel K, Habermehl D, Haberer T, Jakel O, Debus J. Proton and carbon ion radiotherapy for primary brain tumors and tumors of the skull base. Acta Oncol 2013;52:1504–9. https://doi.org/10.3109/0284186X.2013.818255.
[11] Mattke M, Vogt K, Bougatf N, et al. High control rates of proton- and carbon-ion-beam treatment with intensity-modulated active raster scanning in 101 patients with skull base chondrosarcoma at the Heidelberg Ion Beam Therapy Center. Cancer 2018;124:2036–44.
[12] Wink KCJ, Roelofs E, Simone 2nd CB, et al. Photons, protons or carbon ions for stage I non-small cell lung cancer – Results of the multicentric ROCOCO in silico study. Radiother Oncol 2018;128:139–46. https://doi.org/10.1016/j.radonc.2018.02.024.
[13] Jensen AD, Poulakis M, Vanoni V, et al. Carbon ion therapy (C12) for high-grade malignant salivary gland tumors (MSGTs) of the head and neck: do non-ACCs profit from dose escalation? Radiat Oncol 2016;11:90. https://doi.org/10.1186/s13014-016-0657-z.
[14] Jensen AD, Poulakis M, Nikoghosyan AV, et al. High-LET radiotherapy for adenoid cystic carcinoma of the head and neck: 15 years' experience with raster-scanned carbon ion therapy. Radiother Oncol 2016;118:272–80.
[15] Adeberg S, Harrabi SB, Verma V, et al. Treatment of meningioma and glioma with protons and carbon ions. Radiat Oncol 2017;12:193.
[16] Friedrich T, Scholz U, Elsasser T, Durante M, Scholz M. Systematic analysis of RBE and related quantities using a database of cell survival experiments with ion beam irradiation. J Radiat Res 2013;54:494–514.
[17] Tenforde TS, Tenforde SD, Crabtree KE, et al. RBE values for radiation-induced growth delay in rat rhabdomyosarcoma tumors exposed to plateau and peak carbon, neon and argon ions. Int J Radiat Oncol Biol Phys 1981;7:217–22.
[18] Koike S, Ando K, Oohira C, et al. Relative biological effectiveness of 290 MeV/u carbon ions for the growth delay of a radioresistant murine fibrosarcoma. J Radiat Res 2002;43:247–55.
[19] Peschke P, Karger CP, Scholz M, Debus J, Huber PE. Relative biological effectiveness of carbon ions for local tumor control of a radioresistant prostate carcinoma in the rat. Int J Radiat Oncol Biol Phys 2011;79:239–46.
[20] Karger CP, Peschke P, Scholz M, Huber PE, Debus J. Relative biological effectiveness of carbon ions in a rat prostate carcinoma in vivo: comparison of 1, 2, and 6 fractions. Int J Radiat Oncol Biol Phys 2013;86:450–5.
[21] Sorensen BS, Horsman MR, Alsner J, et al. Relative biological effectiveness of carbon ions for tumor control, acute skin damage and late radiation-induced fibrosis in a mouse model. Acta Oncol 2015;54:1623–30.
[22] Glowa C, Karger CP, Brons S, et al. Carbon ion radiotherapy decreases the impact of tumor heterogeneity on radiation response in experimental prostate tumors. Cancer Lett 2016;378:97–103.
[23] Brownstein JM, Wisdom AJ, Castle KD, et al. Characterizing the potency and impact of carbon ion therapy in a primary mouse model of soft tissue sarcoma. Mol Cancer Ther 2018;17:858–68.
[24] Isaacs JT, Heston WD, Weissman RM, Coffey DS. Animal models of the hormone-sensitive and -insensitive prostatic adenocarcinomas, Dunning R-3327-H, R-3327-HI, and R-3327-AT. Cancer Res 1978;38:4353–9.
[25] Walker AM, Suit HD. Assessment of local tumor control using censored tumor response data. Int J Radiat Oncol Biol Phys 1983;9:383–6.
[26] Finney DJ. Statistical Method in Biological Assay 3rd edition London: Charles Griffin, 1978.
[27] Zhao D, Ran S, Constantinescu A, Hahn EW, Mason RP. Tumor oxygen dynamics: correlation of in vivo MRI with histological findings. Neoplasia 2003;5:308–18.
[28] Bassler N, Toftegaard J, Luhr A, et al. LET-painting increases tumour control probability in hypoxic tumours. Acta Oncol 2014;53:25–32.
[29] Mena-Romano P, Cheng C, Glowa C, et al. Measurement of hypoxia-related parameters in three sublines of a rat prostate carcinoma using dynamic (18)F-FMISO-Pet-Ct and quantitative histology. Am J Nucl Med Mol Imaging 2015;5:348–62.
[30] Bendinger AL, Glowa C, Peter J, Karger CP. Photoacoustic imaging to assess pixel-based sO2 distributions in experimental prostate tumors. J Biomed Opt 2018;23:1–11.
[31] Glowa C, Peschke P, Brons S, et al. Carbon ion radiotherapy: impact of tumor differentiation on local control in experimental prostate carcinomas. Radiat Oncol 2017;12:174.
[32] Glowa C, Peschke P, Karger CP, et al. Flow cytometric characterization of tumor subpopulations in three sublines of the Dunning R3327 rat prostate tumor model. Prostate 2013;73:1710–20.
[33] Nomiya T, Tsuji H, Kawamura H, et al. A multi-institutional analysis of prospective studies of carbon ion radiotherapy for prostate cancer: A report from the Japan Carbon ion Radiation Oncology Study Group (J-CROS). Radiother Oncol 2016;121:288–93.